Observation of electroweak Z+2j production at ATLAS

[a.k.a Z-boson production via weak boson fusion]

Andrew Pilkington – University College London

Presented at the 49th Rencontres de Moriond: EW interactions and unified theories

<u>Outline</u>

1) Cross sections and distributions for inclusive Z+2j production
2) Extracting the electroweak Z+2j component

Why bother with electroweak Z+2j production?

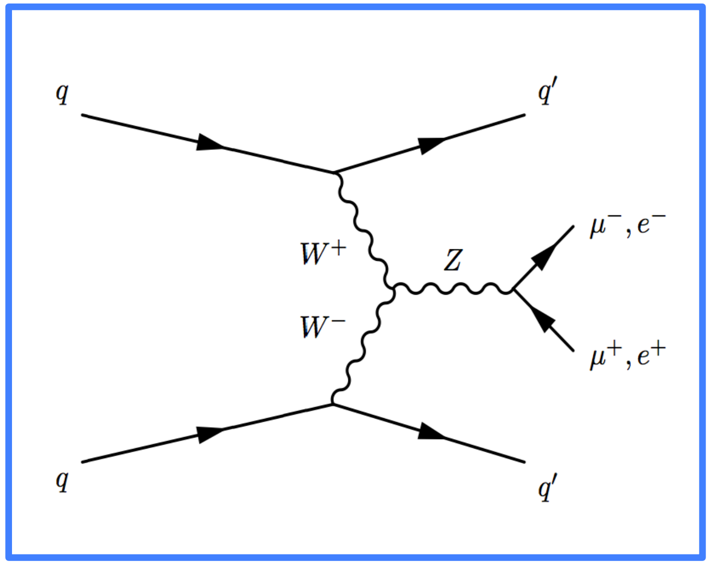

- Weak-boson fusion/scattering plays an important role in Higgs measurements (couplings, ττ) and searches for anomalous quartic gauge couplings.

- Z-production via weak boson fusion is a *standard candle* for these processes
  - first observation of weak boson fusion at a hadron collider
  - a direct test of the ZWW coupling.

Z+2j production at the LHC

Electroweak Zjj

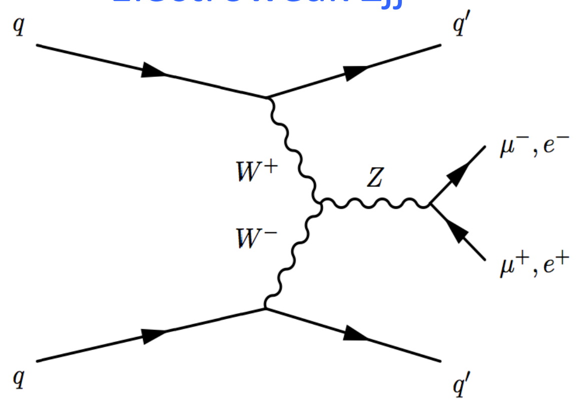

Strong Zjj

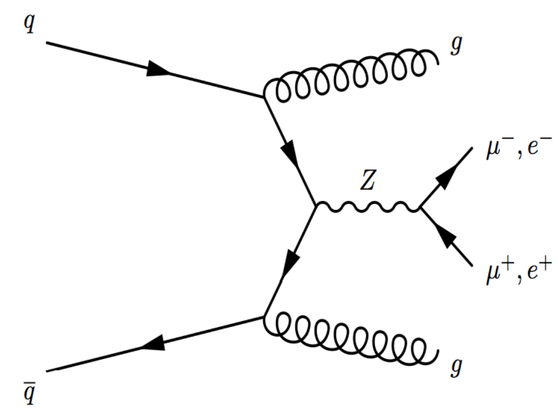

- Electroweak Z+2j production is *rare*: only ~1% of the inclusive Z+2j cross section

- Electroweak Z+2j has two characteristic features:
  - Dijet system covering a large rapidity interval and large invariant mass
  - Little additional jet activity in the rapidity interval

Z+2j production at the LHC

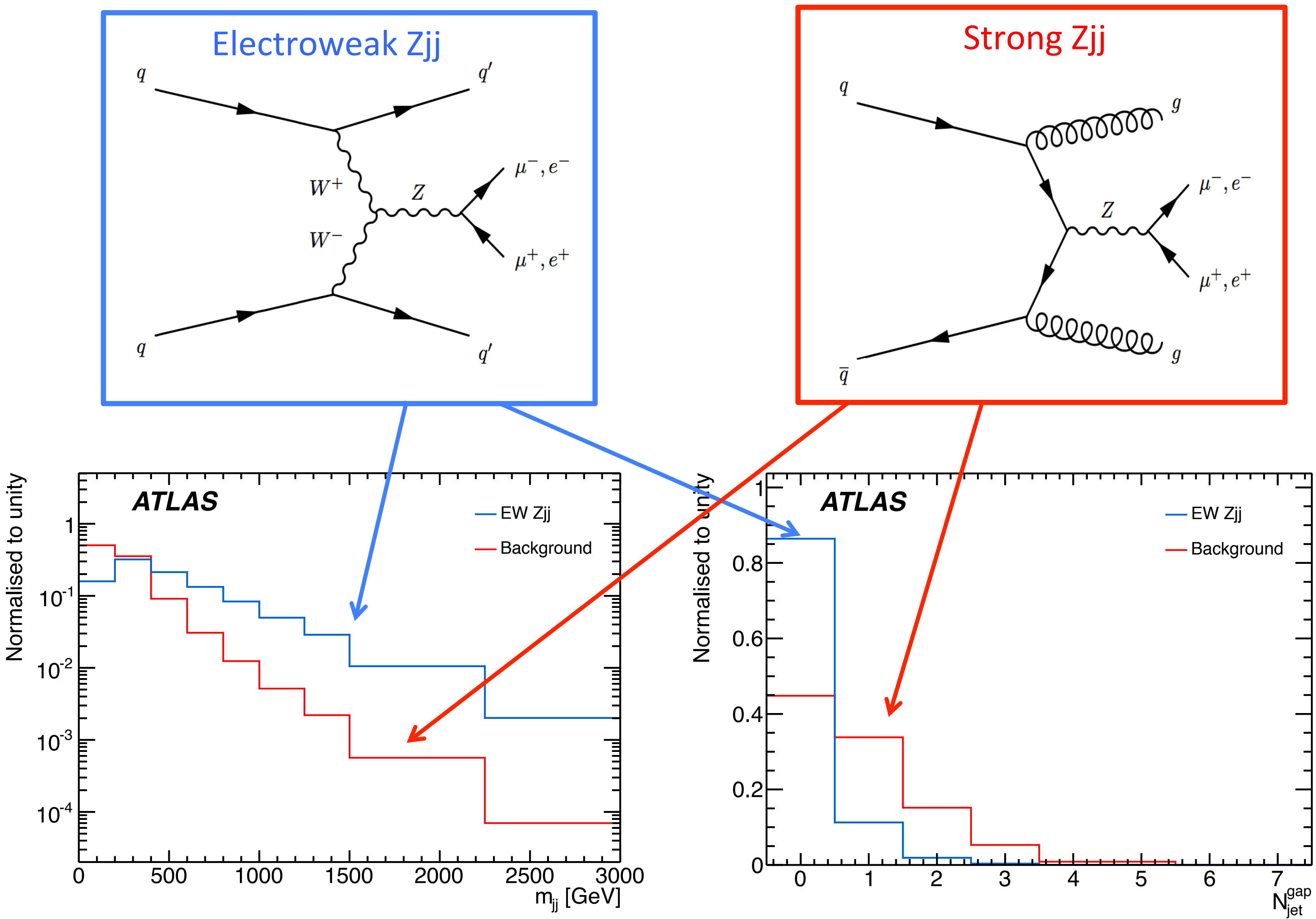

Cross sections and distributions for inclusive Z+2j production

<u>Detector-corrected measurements</u>

1) Cross sections measured in five fiducial regions
2) Differential distributions sensitive to dijet kinematics (m_{jj}, Δy)
3) Differential distributions sensitive to ‘in-gap’ jet activity

Five fiducial regions: different sensitivity to electroweak Zjj

Object	*baseline*	*high-mass*	*search*	*control*	*high-p_T*
Leptons	$\lvert\eta^{\ell}\rvert < 2.47,\ p_T^{\ell} > 25$ GeV				
Dilepton pair	$81 \leq m_{\ell\ell} \leq 101$ GeV				
	—		$p_T^{\ell\ell} > 20$ GeV		—
Jets	$\lvert y^{j}\rvert < 4.4,\ \Delta R_{j,\ell} \geq 0.3$				
	$p_T^{j1} > 55$ GeV				$p_T^{j1} > 85$ GeV
	$p_T^{j2} > 45$ GeV				$p_T^{j2} > 75$ GeV
Dijet system	—	$m_{jj} > 1$ TeV	$m_{jj} > 250$ GeV		—
Interval jets	—		$N_{\text{jet}} = 0$	$N_{\text{jet}} \geq 1$	—
Zjj system	—		$p_T^{\text{balance}} < 0.15$	$p_T^{\text{balance,3}} < 0.15$	—

--- Z-boson selection

--- Baseline jet selection

--- Probe of high-p_T or high-mass

--- Search/control cuts for electroweak extraction

Example of data/simulation in the *baseline* region

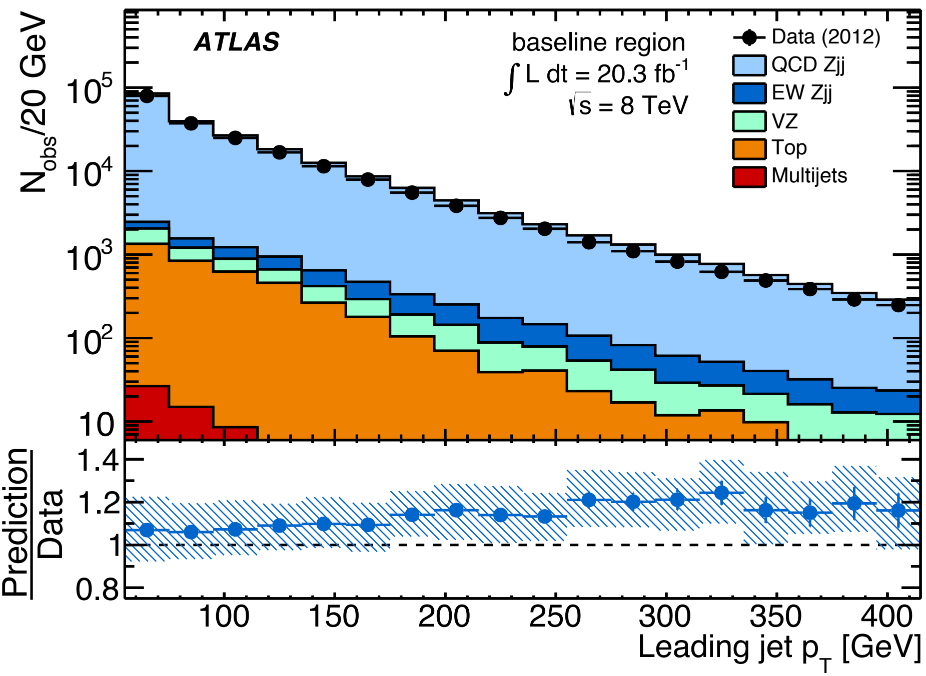

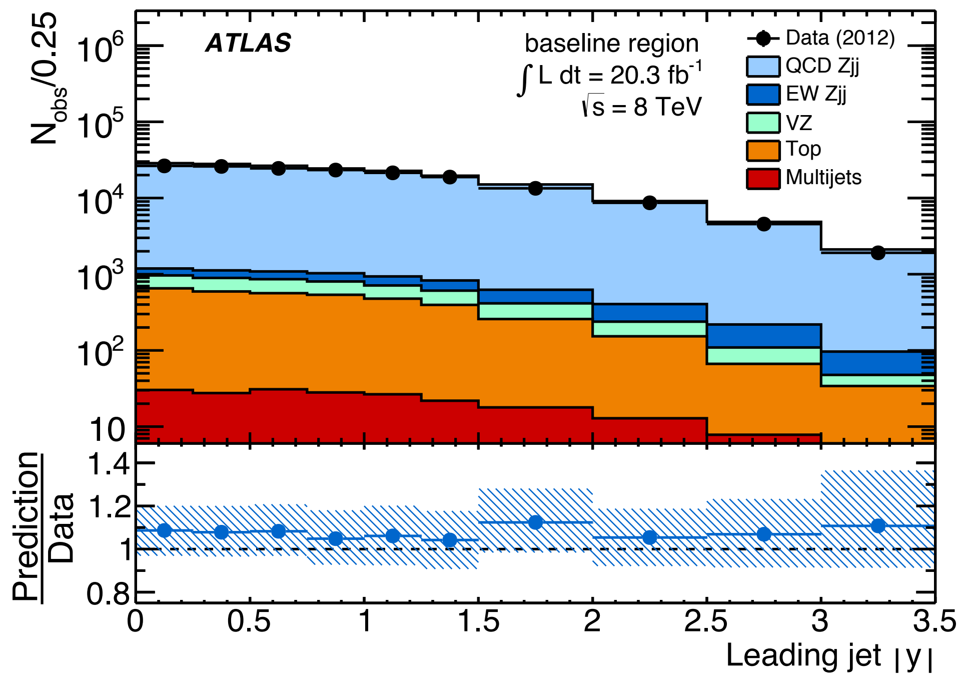

- Small non-Z backgrounds (approx. 2% of total event yield)
- Reasonable agreement between data and simulation

Measurement of inclusive Z+2j cross sections (II)

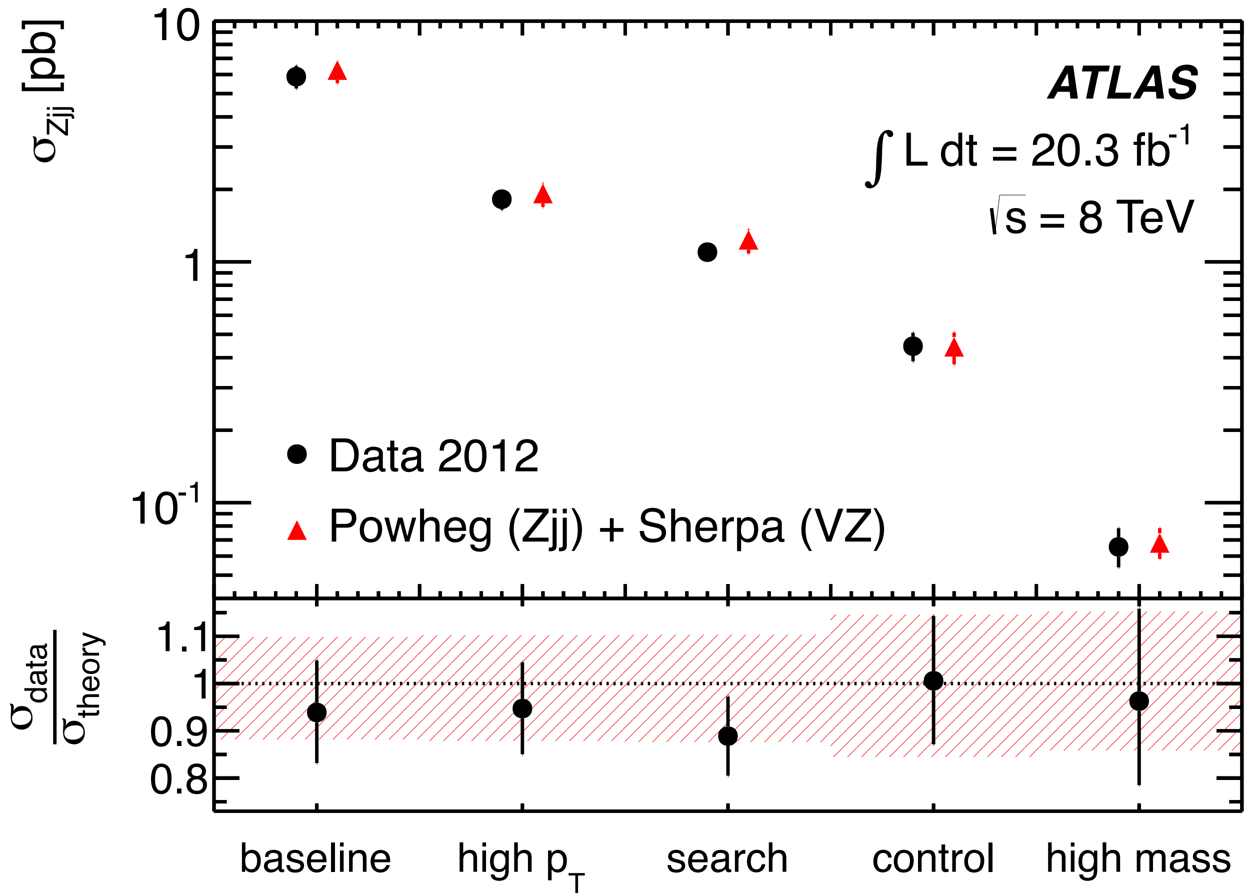

Measure cross section by $\sigma_{\rm fid} = \dfrac{N_{\rm obs} - N_{\rm bkg}}{\int L\,{\rm d}t \cdot \mathcal{C}}$

Measurement of dijet kinematics (unfolded)

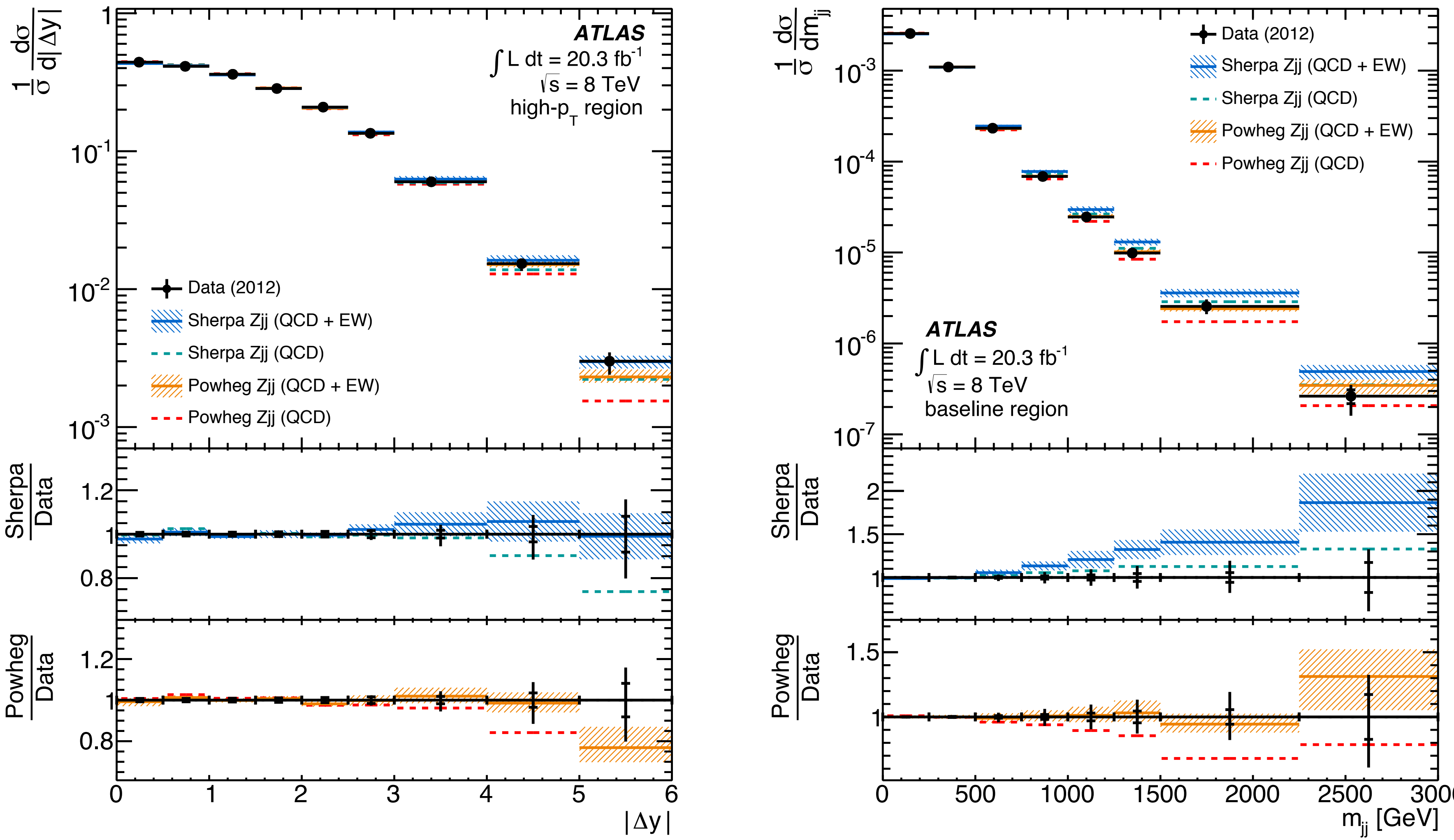

Powheg accurate to next-to-leading order (NLO) in QCD for Z+2j production

Sherpa accurate only to leading order (LO) in QCD for Z+2j production

Measurement of in-gap jet activity (unfolded)

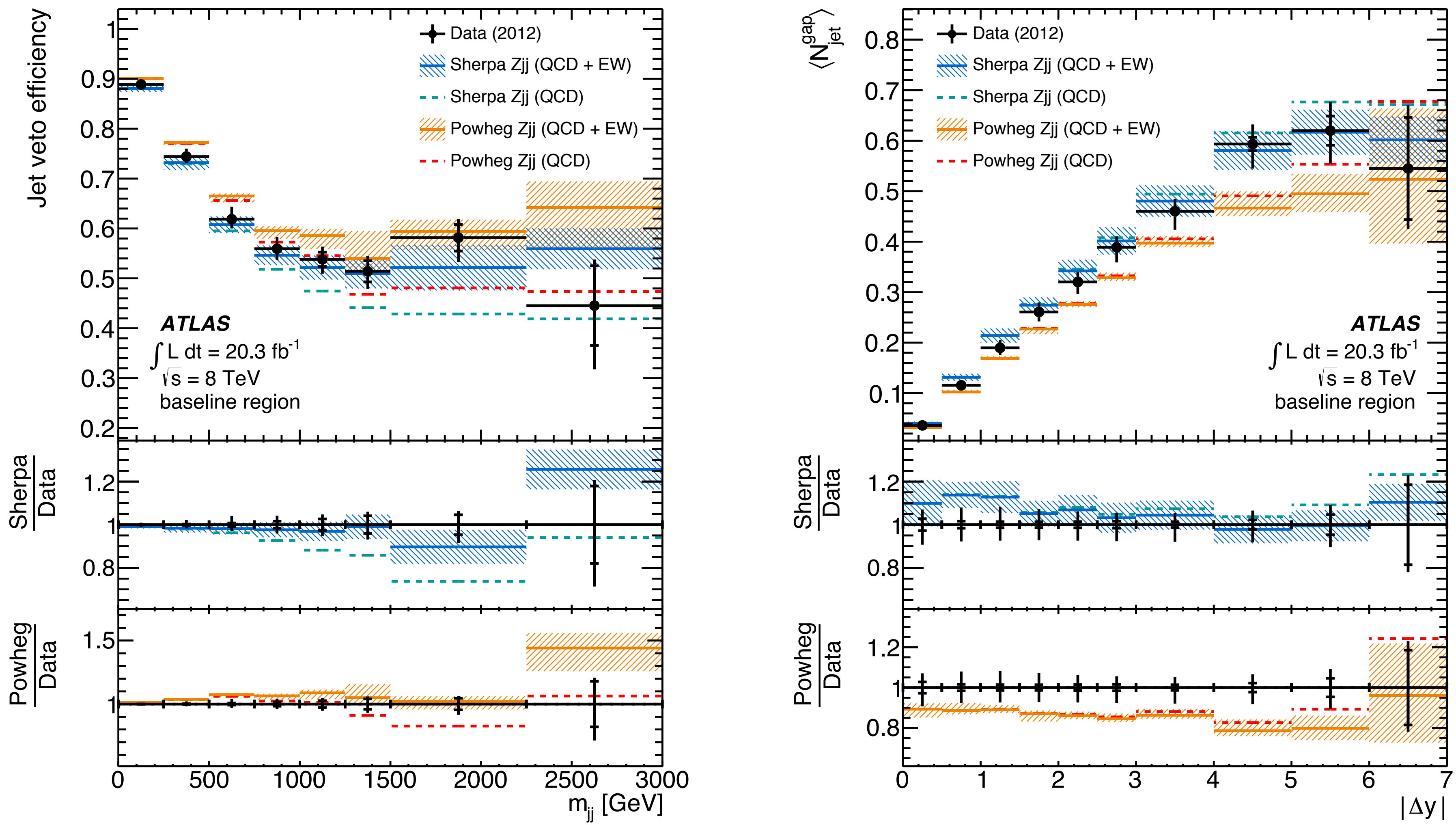

Sherpa accurate to LO in QCD for third and fourth jet emission

Powheg only accurate to LO in QCD for third jet emission

Extracting the electroweak Z+2j component

Extracting the signal - methodology

Electroweak Zjj

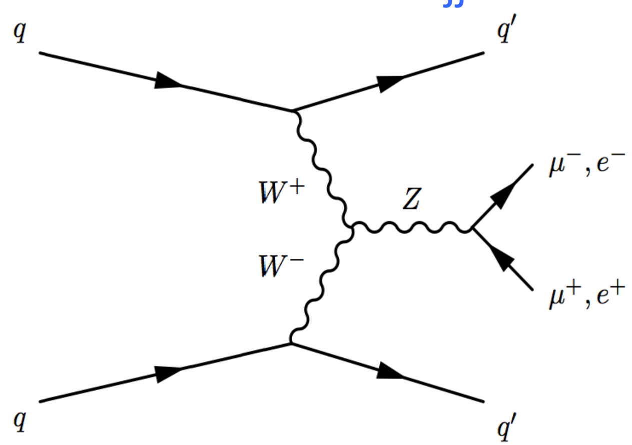

Strong Zjj

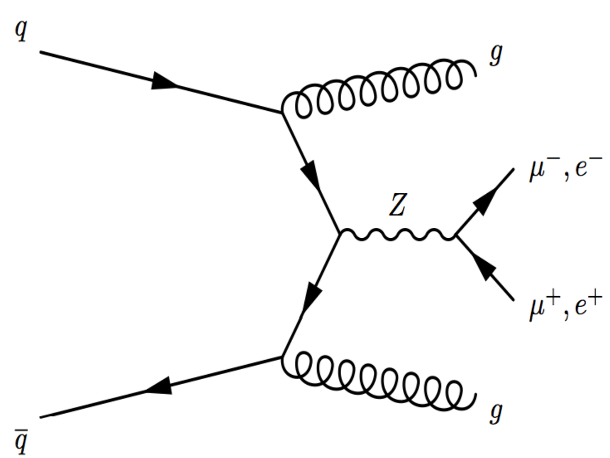

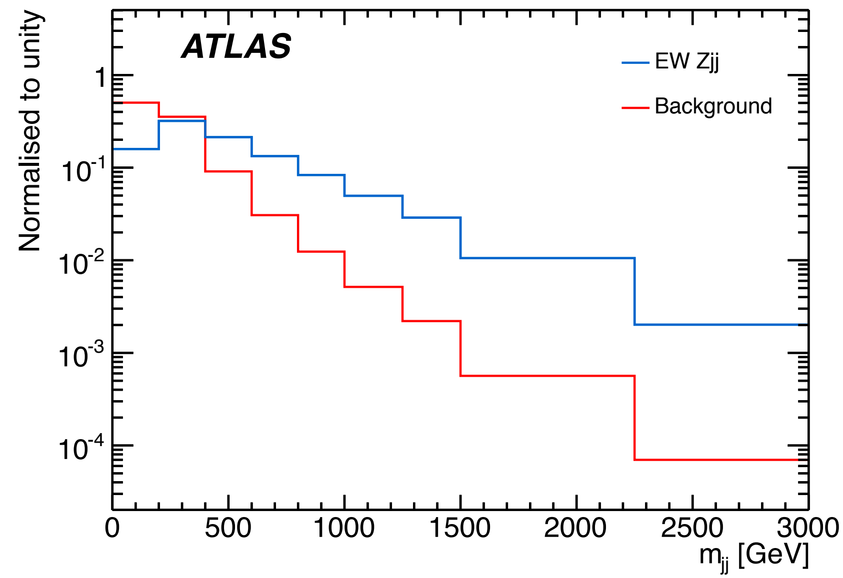

- Electroweak component is extracted by a two template fit to the dijet invariant mass
- This fit is carried out in the *search region*, which has a veto on additional central jet activity

Data-driven constraint for the background model (I)

- Control region defined by <u>reversing</u> the jet veto.
- Basic idea: correct the simulation in the *search* region using the data/MC ratio in the *control* region.
  - Plot shows correction derived for SHERPA
- Added bonus: limits the impact of jet energy scale uncertainties
- Downside: remaining experimental and theoretical uncertainties associated with the extrapolation from *control -> search*

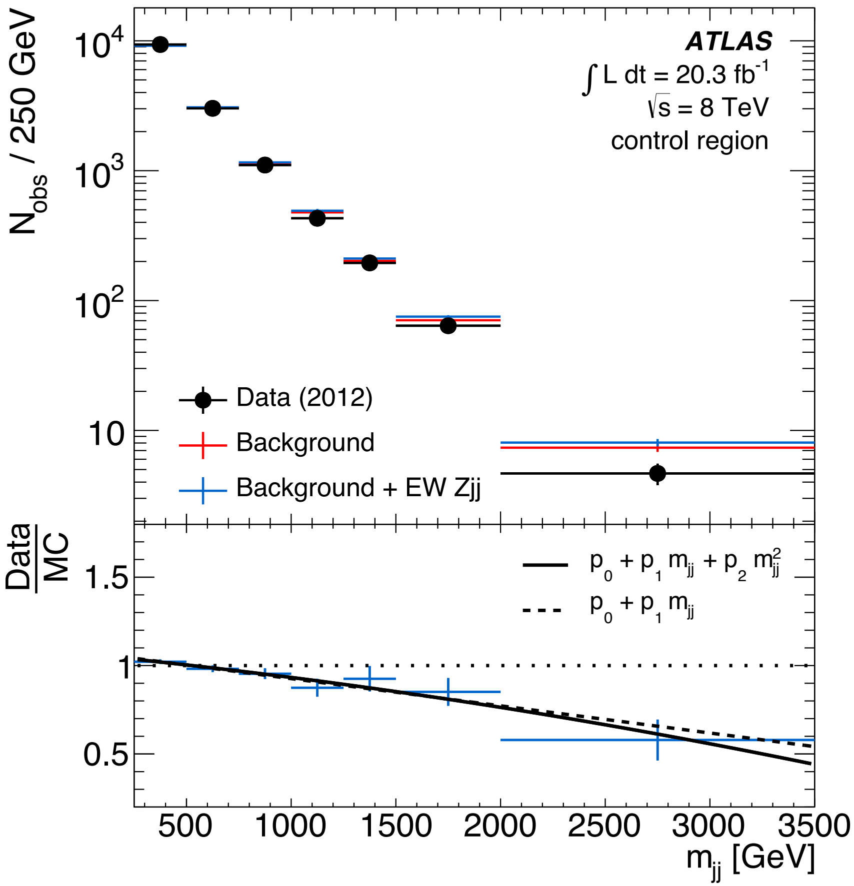

Data-driven constraint for the background model (II)

- Choice of generator checked by using POWHEG (instead of SHERPA) and repeating full analysis chain.
  - Extracted signal yields agree to 0.8%

- Choice of control region validated by splitting it into seven sub-regions,
  - deriving new constraints,
  - repeating full analysis chain.
  - extracted signal yields agree to within 5%.

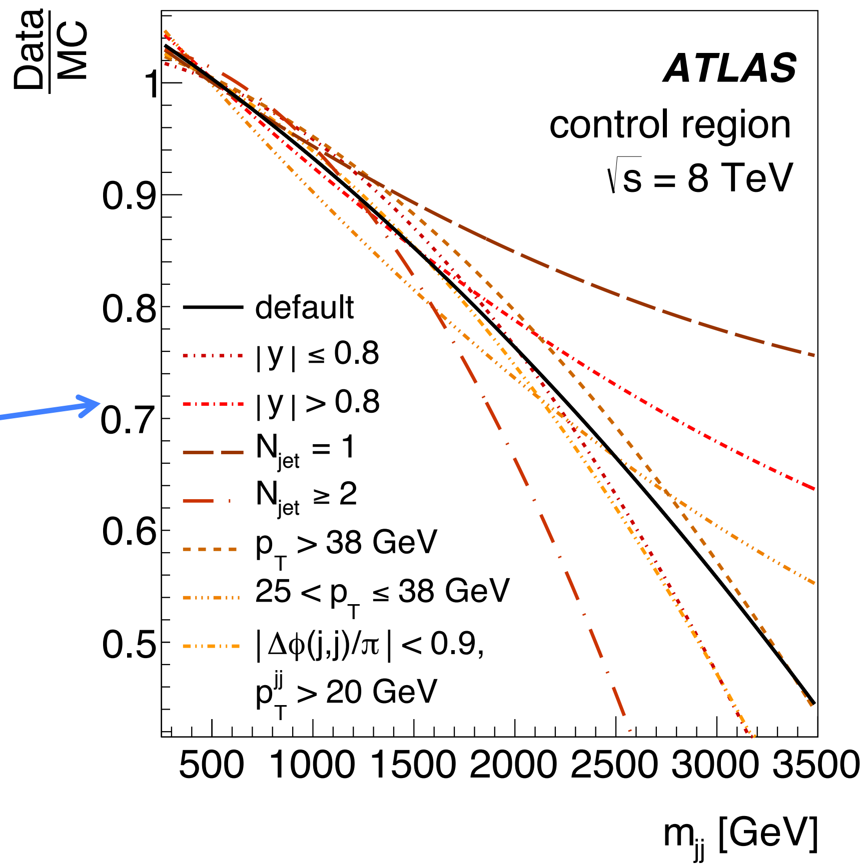

Extracting the signal - results

Fit results

	Electron+muon
Data	32186
MC predicted N_{bkg}	$32600 \pm 2600\,^{+3400}_{-4000}$
MC predicted N_{EW}	$1333 \pm 50 \pm 40$
Fitted N_{bkg}	$30530 \pm 216 \pm 40$
Fitted N_{EW}	$1657 \pm 134 \pm 40$

Background-only hypothesis rejected at greater than 5σ significance

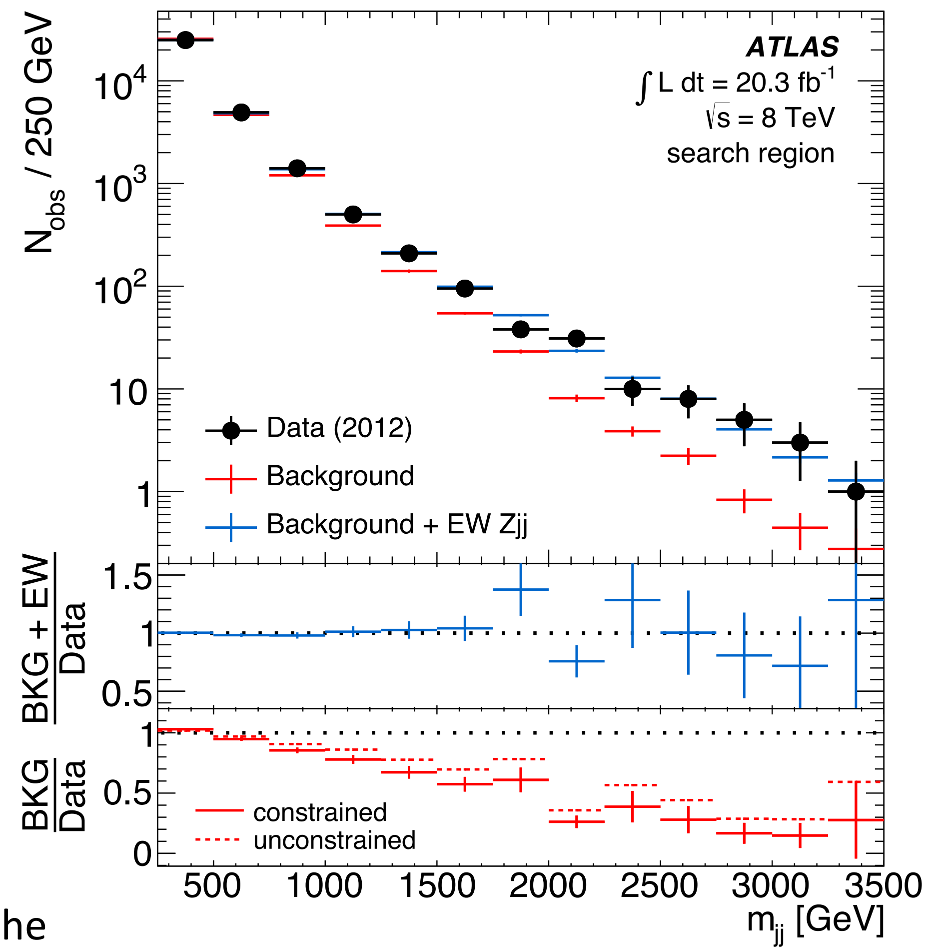

- Extracted yield converted to a cross section in the *search* fiducial region:

$$\sigma_{\mathrm{EW}} = 54.7 \pm 4.6\,(\mathrm{stat})\,^{+9.8}_{-10.4}\,(\mathrm{syst}) \pm 1.5\,(\mathrm{lumi})\ \mathrm{fb}.$$

Breakdown of the electroweak cross section systematics

Source	ΔN_{EW}		$\Delta \mathcal{C}_{\mathrm{EW}}$	
	Electrons	Muons	Electrons	Muons
Lepton systematics	—	—	± 3.2 %	± 2.5%
Control region statistics	± 8.9 %	± 11.2 %	—	—
JES	± 5.6 %		$^{+2.7}_{-3.4}$ %	
JER	± 0.4 %		± 0.8 %	
Pileup jet modelling	± 0.3 %		± 0.3 %	
JVF	± 1.1 %		$^{+0.4}_{-1.0}$ %	
Signal modelling	± 8.9 %		$^{+0.6}_{-1.0}$ %	
Background modelling	± 7.5 %		—	
Signal/background interference	± 6.2 %		—	
PDF	$^{+1.5}_{-3.9}$ %		± 0.1 %	

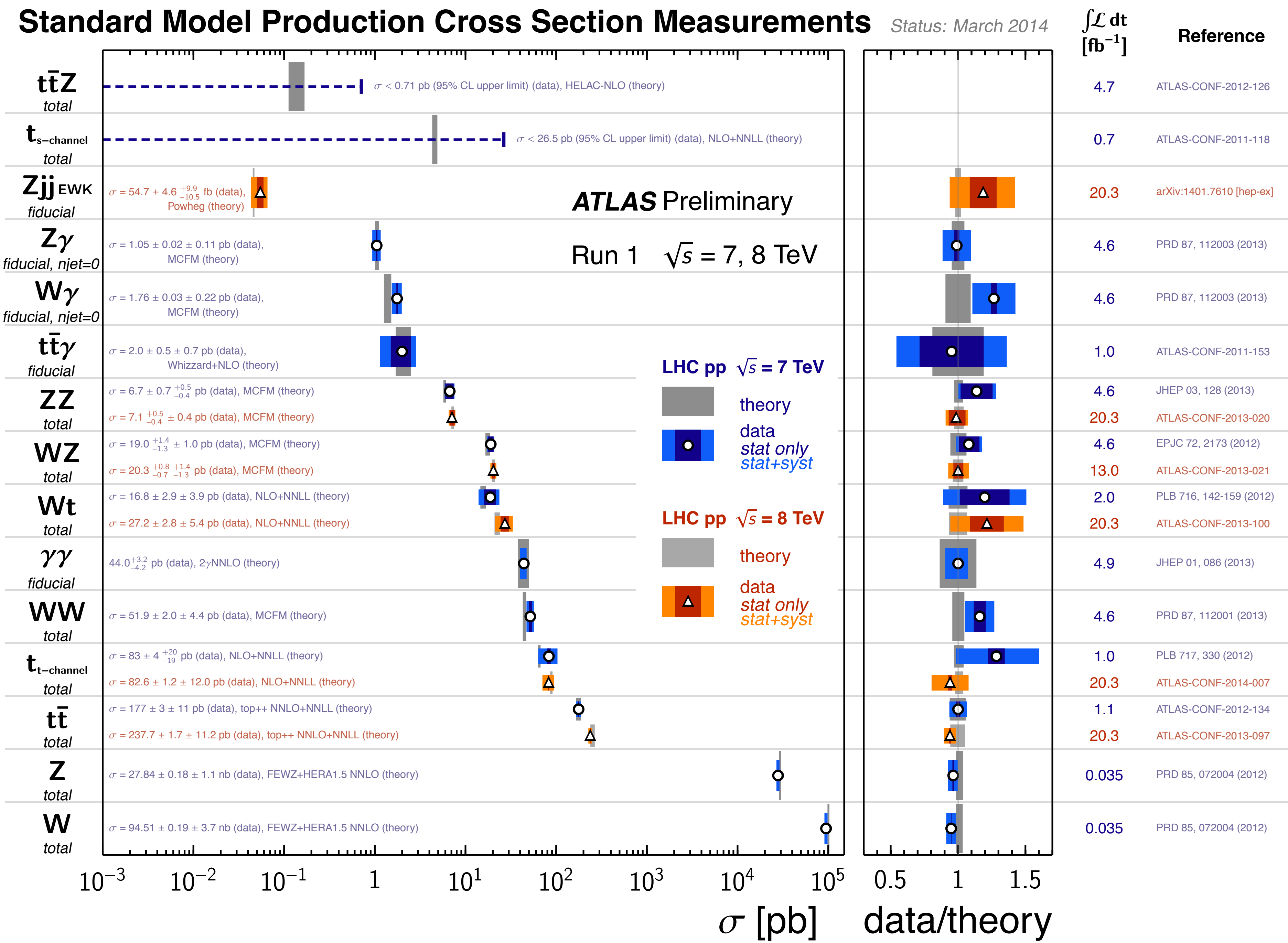
Standard Model Production Cross Section Measurements
Status: March 2014
∫ℒ dt [fb−1]
Reference
tt̄Z total
σ < 0.71 pb (95% CL upper limit) (data), HELAC-NLO (theory)
4.7
ATLAS-CONF-2012-126
ts−channel total
σ < 26.5 pb (95% CL upper limit) (data), NLO+NNLL (theory)
0.7
ATLAS-CONF-2011-118
Zjj EWK fiducial
σ = 54.7 ± 4.6 +9.9 −10.5 fb (data), Powheg (theory)
20.3
arXiv:1401.7610 [hep-ex]
Zγ fiducial, njet=0
σ = 1.05 ± 0.02 ± 0.11 pb (data), MCFM (theory)
4.6
PRD 87, 112003 (2013)
Wγ fiducial, njet=0
σ = 1.76 ± 0.03 ± 0.22 pb (data), MCFM (theory)
4.6
PRD 87, 112003 (2013)
tt̄γ fiducial
σ = 2.0 ± 0.5 ± 0.7 pb (data), Whizzard+NLO (theory)
1.0
ATLAS-CONF-2011-153
ZZ total
σ = 6.7 ± 0.7 +0.5 −0.4 pb (data), MCFM (theory)
4.6
JHEP 03, 128 (2013)
σ = 7.1 +0.5 −0.4 ± 0.4 pb (data), MCFM (theory)
20.3
ATLAS-CONF-2013-020
WZ total
σ = 19.0 +1.4 −1.3 ± 1.0 pb (data), MCFM (theory)
4.6
EPJC 72, 2173 (2012)
σ = 20.3 +0.8 −0.7 +1.4 −1.3 pb (data), MCFM (theory)
13.0
ATLAS-CONF-2013-021
Wt total
σ = 16.8 ± 2.9 ± 3.9 pb (data), NLO+NNLL (theory)
2.0
PLB 716, 142-159 (2012)
σ = 27.2 ± 2.8 ± 5.4 pb (data), NLO+NNLL (theory)
20.3
ATLAS-CONF-2013-100
γγ fiducial
44.0 +3.2 −4.2 pb (data), 2γNNLO (theory)
4.9
JHEP 01, 086 (2013)
WW total
σ = 51.9 ± 2.0 ± 4.4 pb (data), MCFM (theory)
4.6
PRD 87, 112001 (2013)
tt−channel total
σ = 83 ± 4 +20 −19 pb (data), NLO+NNLL (theory)
1.0
PLB 717, 330 (2012)
σ = 82.6 ± 1.2 ± 12.0 pb (data), NLO+NNLL (theory)
20.3
ATLAS-CONF-2014-007
tt̄ total
σ = 177 ± 3 ± 11 pb (data), top++ NNLO+NNLL (theory)
1.1
ATLAS-CONF-2012-134
σ = 237.7 ± 1.7 ± 11.2 pb (data), top++ NNLO+NNLL (theory)
20.3
ATLAS-CONF-2013-097
Z total
σ = 27.84 ± 0.18 ± 1.1 nb (data), FEWZ+HERA1.5 NNLO (theory)
0.035
PRD 85, 072004 (2012)
W total
σ = 94.51 ± 0.19 ± 3.7 nb (data), FEWZ+HERA1.5 NNLO (theory)
0.035
PRD 85, 072004 (2012)
ATLAS Preliminary
Run 1 √s = 7, 8 TeV
LHC pp √s = 7 TeV
theory
data
stat only
stat+syst
LHC pp √s = 8 TeV
theory
data
stat only
stat+syst
10−3 10−2 10−1 1 10¹ 10² 10³ 10⁴ 10⁵
σ [pb]
0.5 1 1.5
data/theory

Summary

- Inclusive Zjj production measured using ATLAS data
  - Cross sections in five fiducial regions
  - Differential distributions fully corrected for detector effects

- Observation of electroweak Zjj production at ATLAS
  - *A benchmark process for future studies of weak-boson fusion at the LHC*
  - Background-only hypothesis rejected at greater than 5σ
  - Cross section measured in two fiducial regions. Excellent agreement with NLO.
  - First limits placed on anomalous triple gauge couplings using weak boson fusion.

- For further information: arXiv:1401.7610

Backup

Process composition in each fiducial region

	Composition (%)				
Process	*baseline*	*high-p_T*	*search*	*control*	*high-mass*
Strong Zjj	95.8	94.0	94.7	96.0	85
Electroweak Zjj	1.1	2.1	4.0	1.4	12
WZ and ZZ	1.0	1.3	0.7	1.4	1
$t\bar{t}$	1.8	2.2	0.6	1.0	2
Single top	0.1	0.1	< 0.1	< 0.1	< 0.1
Multijet	0.1	0.2	< 0.1	0.2	< 0.1
WW, W+jets	< 0.1	< 0.1	< 0.1	< 1.1	< 0.1

- Small non-Z background contributions (~2%)
- Cross section determined by $\sigma_{\text{fid}} = \frac{N_{\text{obs}} - N_{\text{bkg}}}{\int L\,\text{d}t \cdot \mathcal{C}}$, where L is the luminosity and C corrects for detector effects.

Cross section measurement and aTGC limits

- Measured cross section:

$$\sigma_{\mathrm{EW}} = 54.7 \pm 4.6\,(\mathrm{stat})\,^{+9.8}_{-10.4}\,(\mathrm{syst}) \pm 1.5\,(\mathrm{lumi})\,\mathrm{fb}.$$

- Theory prediction:

$$\sigma_{\mathrm{EW}} = 46.1 \pm 0.2\,(\mathrm{stat})\,^{+0.3}_{-0.2}\,(\mathrm{scale}) \pm 0.8\,(\mathrm{PDF}) \pm 0.5\,(\mathrm{model})\;\mathrm{fb}$$

- Limits on anomalous triple gauge couplings:

aTGC	$\Lambda = 6$ TeV (obs)	$\Lambda = 6$ TeV (exp)	$\Lambda = \infty$ (obs)	$\Lambda = \infty$ (exp)
$\Delta g_{1,Z}$	[−0.65, 0.33]	[−0.58, 0.27]	[−0.50, 0.26]	[−0.45, 0.22]
λ_Z	[−0.22, 0.19]	[−0.19, 0.16]	[−0.15, 0.13]	[−0.14, 0.11]

$$\frac{\mathcal{L}}{g_{WWZ}} = i\left[g_{1,Z}\left(W^{\dagger}_{\mu\nu}W^{\mu}Z^{\nu} - W_{\mu\nu}W^{\dagger\mu}Z^{\nu}\right) + \kappa_Z W^{\dagger}_{\mu}W_{\nu}Z^{\mu\nu} + \frac{\lambda_Z}{m_W^2}W^{\dagger}_{\rho\mu}W^{\mu}_{\nu}Z^{\nu\rho}\right]$$

Why bother with weak boson fusion?

Higgs measurements

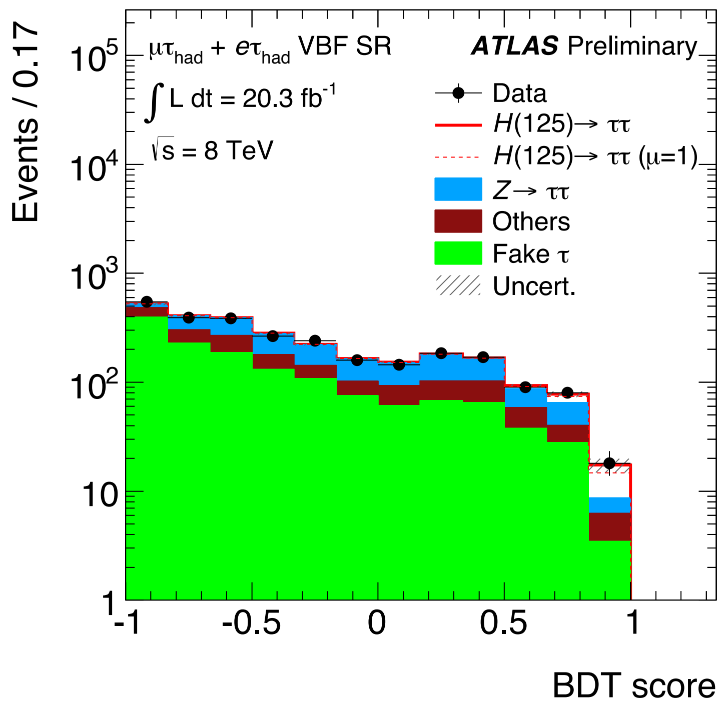

Quartic gauge couplings?

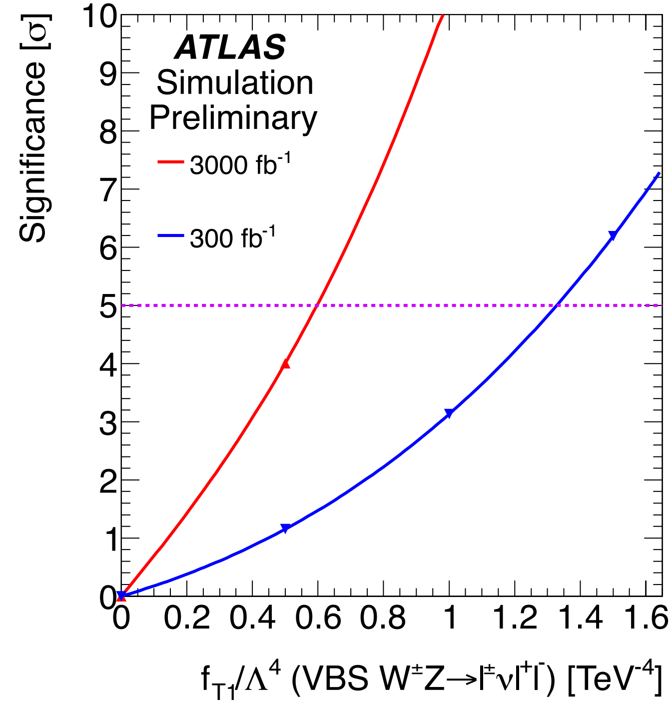

- In the LHC Run-II, weak boson fusion is due to play a major part in tests of the electroweak sector of the Standard Model:
  - Higgs production via weak boson fusion and HWW coupling determination
  - Weak boson scattering measurements and searches for anomalous gauge couplings

Validation of control region constraint

- Choice of control region was validated by splitting it into seven sub-regions
  - All these regions are signal suppressed
- Can use orthogonal sub-regions to see if the reweighting function derived on one region improves the agreement between simulation and data in another region
- Agreement improved in all cases,
- Example, shown here is for orthogonal sub-regions that differ in the third jet transverse momentum.